NASA TECHNICAL TRANSLATION NASA TT F-15,039

COMPUTATION OF UNSTEADY AERODYNAMIC FORCES ON HELICOPTER ROTOR BLADES

J.-J. Costes

(NASA-TT-F-15039) COMPUTATION OF UNSTEADY AERODYNAMIC FORCES ON HELICOPTER ROTOR BLADES (Kanner (Leo) Associates) 34 p HC $3.75 CSCL 01C

N73-28981

Unclas G3/02 11332

Translation of "Calcul des forces aérodynamiques instationnaires sur les pales d'un rotor d'hélicoptère," La Recherche Aérospatiale, No. 2, 1972, pp. 91-106

NATIONAL AERONAUTICS AND SPACE ADMINISTRATION
WASHINGTON, D.C. 20546 AUGUST 1973

COMPUTATION OF UNSTEADY AERODYNAMIC FORCES ON HELICOPTER ROTOR BLADES

Jean-Joël Costes
Office National d'Études et de Recherches Aérospatiales

Introduction

/3-2*

In an article in La Recherche Aérospatiale [1] R. Dat proposed a new method to calculate the unsteady aerodynamic forces acting on helicopter blades. Based on the use of the theory of pressure doublets, this method permits introducing the effects of air compressibility in a rigorous manner. A practical application is set forth here, and the numerical results are compared with the results provided by the vortex theory and with experimental results.

I. General Equations

I, 1. Case of the Incompressible Fluid

Let us consider a perfect fluid endowed with a uniform motion of velocity U_∞. An obstacle placed in the fluid modifies the velocity at every point in space. At P velocity becomes $U(P) = U_\infty + V(P)$:

The following restrictions are imposed on the disturbance velocity V(P):

1) V(P) small compared to U_∞.

---

* Numbers in the margin indicate pagination in the foreign text.

2) There exists $\phi(P)$, which is a scalar function of the point P such that $V(P) = \text{grad}[\phi(P)]$; $\phi(P)$ is the velocity potential.

In the case of an incompressible fluid, function $\phi(P)$ must moreover verify equations

$$\frac{\partial^2\varphi}{\partial x^2} + \frac{\partial^2\varphi}{\partial y^2} + \frac{\partial^2\varphi}{\partial z^2} = 0 \quad \text{conservation of mass,} \tag{1}$$

$$\rho_\infty \frac{d\varphi}{dt} = -[p - p_\infty] \quad \text{[see ref. 1] motion equation,} \tag{2}$$

with:

ρ_∞ = density, p_∞ = upstream pressure at infinity,

p = pressure at the point involved.

Equations (1) and (2) are written with an absolute coordinate sytem Oxyz.

The presence of $\frac{d\phi}{dt}$ particular derivative of ϕ, in Eq. (2), suggests introducing the scalar function

$$\psi(P) = \frac{d\varphi}{dt}(P).$$

Fluid acceleration, being yielded by $\gamma(P) = \frac{dV}{dt} = \frac{d}{dt}[\text{grad } \phi] \sim \text{grad } [\psi(P)]$, $\psi(P)$ is an acceleration potential. It must moreover verify relations

$$\gamma(P) = \text{grad } [\psi(P)], \tag{3}$$

$$\frac{\partial^2\psi}{\partial x^2} + \frac{\partial^2\psi}{\partial y^2} + \frac{\partial^2\psi}{\partial z^2} = 0 \quad \text{obtained by derivation from (1),} \tag{4}$$

$$\psi = -\frac{[p - p_\infty]}{\rho_\infty} \quad \text{analogous to Eq. (2).} \tag{5}$$

Since Eq. (4) is linear, any linear combination of particular solutions verifies (4). Thus, for example, the potential of a source (or of an electric charge) placed at P_0 responds to equation (4) at every point in space other than P_0. The nature of the singularity at P_0 makes the potential source very suitable for the solution of a thickness problem. Another particular solution, the pressure-doublet potential, obtained by causing a source and a well of equal intensity and inversely proportional to the distance to approach one another according to the direction $\vec{n}_0$, is used in the case of a lift problem. One shows that the potential obtained has a limit. This limit still satisfies Eq. (4). The potential, at moment t at the point P, for an intensity doublet q(t) situated at the same moment t at point P_0 is yielded by the expression (Fig. 1).

$$\psi(P,t) = -q(t)\frac{\overrightarrow{P_0P}\cdot\vec{n}_0}{4\pi|\overrightarrow{P_0P}|^3}. \tag{6}$$

with $D = |P_0P|$ and θ angle oriented from $\overrightarrow{P_0P}$ to $\vec{n}_0$, one obtains the equivalent expression.

$$\psi(P,t) = -\frac{q(t)\cos\theta}{4\pi D^2}. \tag{7}$$

This potential when D approaches 0 now has to be interpreted. If one considers a surface on which a distribution of doublets with axes perpendicular to the surface and of intensity q(P, t) is given, it is possible [2] to show that q(P,t) is linked to pressure difference Δp through the surface by the expression (Fig. 2). /3-3

$$q(P,t) = \frac{\Delta p(P,t)}{\rho_\infty}. \tag{8}$$

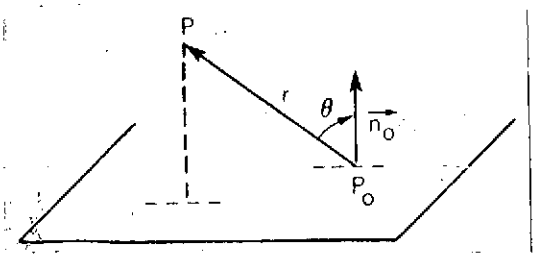

Fig. 1.

Expression (8) yields a simple interpretation of the lifting surface since the latter can be represented by a sheet of doublets with axes perpendicular to the surface and of intensity proportional to $\Delta p(P,t)$. In the case of a wing with a large aspect ratio the main interest may lie not in the distribution of Δp at every point of the wing, but on the distribution of lift spanwise.

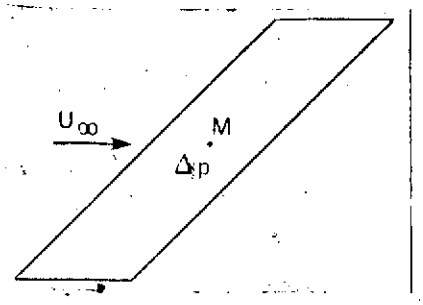

Fig. 2.

If the reduced motion frequency of the wing is low, if deformation along the chord is negligible and if there is no control deflection, this lift can be determined schematizing the wing by means of a lifting line situated in the forward quarter.

The intensity of the doublets placed on this lifting line is yielded by

$$q(t,y) = \int_{x_2}^{x_1} \Delta p(t,y,x)\, dx, \qquad (9)$$

which amounts to linking this intensity to the pressure integral on an elemental section.

The acceleration potential at any given point in space is the sum of the potential created by each doublet:

$$\varphi(P,t) = \int_{y_2}^{y_1} \frac{-q(t,y)\cos\theta(y,t)}{4\pi D^2_{(y,t)}}\, dy, \qquad (10)$$

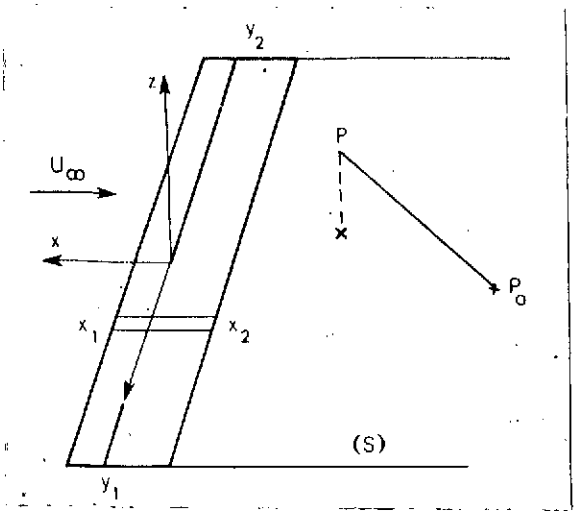

Fig. 3.

expression (10) being obtained substituting (9) in expression (7) and integrating over the entire length of the
Actually one is not seeking to obtain the acceleration of the fluid but its velocity. At about a constant the velocity potential is yielded by

$$\varphi(P,t) = \int_{-\infty}^{t} \psi(P,\tau)\,d\tau.$$

Replacing $\psi(p,t)$ by its value given by (10) we have:

$$\varphi(P,t) = \int_{-\infty}^{t} d\tau \int_{y_2}^{y_1} \frac{-q(\tau,y)\cos\theta(y,\tau)}{4\pi D^2_{(y,\tau)}}\,dy. \qquad (11)$$

It is therefore necessary to know the geometric locus (S) /3-4
(Fig. 3) of the lifting line which shifts with time. For a wing in horizontal motion at a constant velocity U_∞ we have $x = -U_\infty (t - \tau)$ and (11) becomes

$$\varphi(P,t) = -\frac{1}{U_\infty}\int_{y_2}^{y_1} dy \int_{-\infty}^{x} \frac{q(P_0)\cos\theta_{(P_0P)}}{4\pi D^2_{(P_0P)}}\,dx. \qquad (12)$$

We thus obtain a surface integral extending to the portion of the plane swept by the lifting line up to moment t.

When P_0 is a point of (S), $D^2_{(P_0P)}$ can cancel out. To interpret $\phi(P,t)$ as P approaches the geometric locus (S) (Fig. 4)

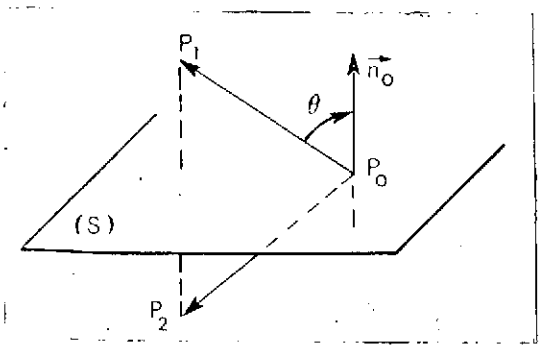

Fig. 4.

we consider two points P_1 and P_2 symmetrical with respect to (S). Formula (7) shows that the potentials created at these two points by a doublet of axis $\vec{n}_0$ perpendicular to (S) are identical in absolute value and of opposite sign, since θ is an oriented angle.

Integrating over (S) using formula (12) one obtains $\phi(P_s) = -\phi(P_1)$ whence: potential ϕ is antisymmetric and discontinuous with respect to (S). Their fluid disturbance velocity is yielded by $V = \text{grad}\ (\phi)$.

Let us consider four neighboring and symmetrical points with respect to (S) (Fig. 5). By making the two points situated on the same side of (S) it is seen that opposite values are obtained for the velocity components parallel to plane (S) and an unchanged perpendicular component. The same reasoning applies to a nonplanar surface (S), since locally the latter may be likened to a tangent plane. (S) thus appears as a discontinuity zone for the disturbance velocity components situated on the plane tangent to (S). The locus of this discontinuity, which can be likened to a sheet of vortices either free or linked to the wing (Fig. 6) and (S), and which has been defined as a geometric locus of the lifting line constitutes the wake of the wing.

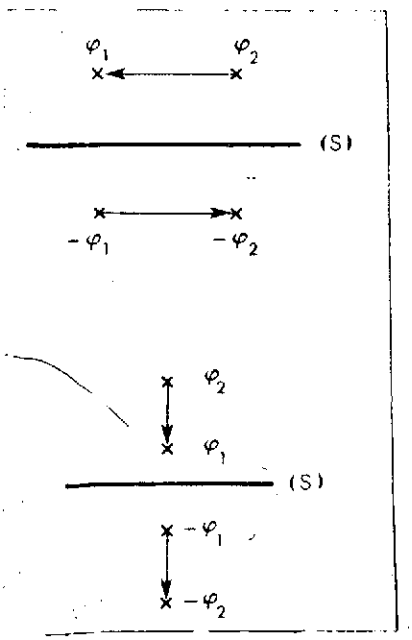

Fig. 5.

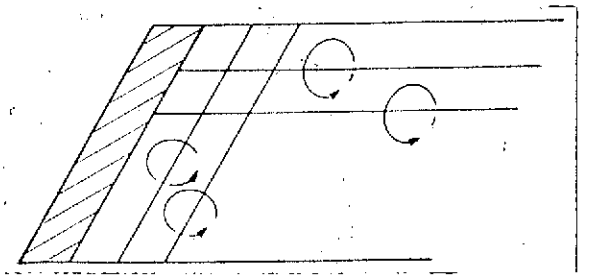

Fig. 6.

I,2. Case of the Compressible Fluid

The same approach, which was used in the preceding paragraph to go from the velocity potential to the acceleration potential, is encountered here. In a linearized compressible fluid, the acceleration potential is the solution of Eq. (13), which expresses conservation of mass:

$$\frac{\partial^2 \psi}{\partial x^2} + \frac{\partial^2 \psi}{\partial y^2} + \frac{\partial^2 \psi}{\partial z^2} - \frac{1}{a^2}\frac{d^2 \psi}{dt^2} = 0; \qquad (13)$$

a is the speed of sound in the medium involved, Oxyz is an absolute coordinate system.

In the first approximation the equation of motion is given by the expression

$$\psi = -\frac{[p - p_\infty]}{\rho_\infty}, \qquad (14)$$

where p_∞ and ρ_∞ are the upstream pressure and density at infinity. Expressions (13) and (14) are written in an absolute coordinate /3-5 system Oxyz.

Eq. (13) leads to the introduction of a delayed potential.

As in the preceding paragraph, the linearity of the equation permits the construction of a solution by superposition of basic solutions. The acceleration doublet, which is equivalent to a lifting surface element, is particularly suited to the lift problem.

The potential of the motion doublet is yielded by (15) [1]:

$$\varphi(P,t) = \frac{dq}{d\tau}(\tau)\,\frac{\vec{n}_0\cdot\vec{D}}{-4\pi|D|^2 a\left[1-\frac{\vec{V}_0\cdot\vec{D}}{a|D|}\right]^2} + \frac{q(\tau)(\vec{D}\cdot\vec{\gamma}_0)(\vec{n}_0\cdot\vec{D})}{-4\pi a^2|D|^3\left[1-\frac{\vec{V}_0\vec{D}}{a|D|}\right]^3} + q(\tau)\,\frac{\frac{d\vec{n}_0}{d\tau}\cdot\vec{D}}{-4\pi|D|^2 a\left[1-\frac{\vec{V}_0\cdot\vec{D}}{a|D|}\right]^2} + q(\tau)\,\frac{\left[(a^2-|V_0|^2)(\vec{n}_0\cdot\vec{D})+(\vec{V}_0\cdot\vec{D}-a|D|)(\vec{V}_0\cdot\vec{n}_0)\right]}{-4\pi a^2|D|^3\left[1-\frac{\vec{V}_0\vec{D}}{a|D|}\right]^3} \qquad (15)$$

(1)

In this formula $\overrightarrow{P_0P} = \vec{D}$ (Fig. 7),

$\vec{V}_0$ is the velocity of P_0 at moment τ,

$dq/d\tau(\tau)$ is the derivative of the doublet intensity at instant τ;

τ is determined by expression (16)

$$t-\tau = \frac{|D|}{a}. \qquad (16)$$

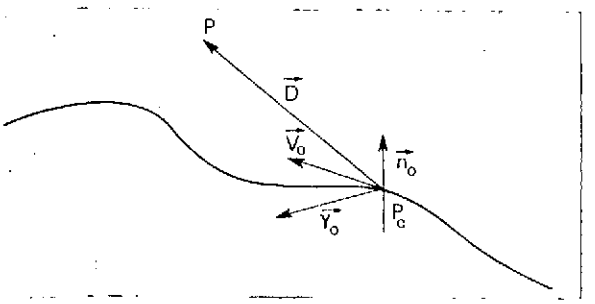

Fig. 7.

The potential created at P at moment t by a doublet placed at P_0 is determined by the intensity of the doublet at moment τ.

The delayed potential expresses the fact that the waves are displaced at finite velocity, a. One goes from the

[1] In the article of Rech. Aérosp., No. 2, 1972 (March-April), pp. 91-106 the term at $d\vec{n}_0/d\tau$ of formulas (15) and (17) was omitted. The results presented here take it into account.

acceleration potential to the velocity potential as in the preceding paragraph, i.e., by an integration, from $-\infty$ to τ_1, where τ_1 is yielded by

$$t - \tau_1 = \frac{\left|\overrightarrow{P_0(\tau_1)P}\right|}{a}.$$

The waves emitted by the doublet between t and τ_1 have not as yet had time to reach point P. The interpretation of the wake as a discontinuity zone of the tangential components of velocity call for $\overrightarrow{n_0}$ to be taken as normal to (S). The demonstration is made in a manner similar to the one given for an incompressible medium. The presence of the acceleration term γ_0 introduces only a few complications. In the case of a helicopter or of a propeller whose blades are schematized by a lifting line (Fig. 8) the velocity potential at point M at moment t is, taking into account the notice $(\overrightarrow{V_0}.\overrightarrow{n_0}) = 0$, yielded by expression (17). It is obtained in the same manner as (11) from a kernel (15), with a change of variable:

$$\tau_0 = \tau - \frac{|D|}{a}, \text{ d'où } d\tau_0 = \left[1 - \frac{\vec{V}_0.\vec{D}}{a|D|}\right] d\tau;$$

it becomes:

$$\varphi(P,t) = \int_{R_0}^{R_1} \int_{-\infty}^{\tau_1(r)} \frac{\left(\frac{dq}{d\tau}(r,\tau)\right)_{\tau=\tau_0} (\vec{n_0}.\vec{D})}{-4\pi a|D|^2\left[1 - \frac{\vec{V_0}.\vec{D}}{a|D|}\right]} d\tau_0 dr + \int_{R_0}^{R_1} \int_{-\infty}^{\tau_1(r)} \frac{q(r,\tau_0).\left(\vec{D}.\left(\frac{d\vec{n_0}}{d\tau}\right)_{\tau=\tau_0}\right)}{-4\pi a|D|^2\left[1 - \frac{\vec{V_0}.\vec{D}}{a|D|}\right]} d\tau_0 dr \quad (17)\ (2)$$

(17)

---

[2] In the article of Rech, Aerosp., No. 2, 1972 (March-April), pp. 91-106 the term $d\vec{n_0}/d\tau$ of formulas (15) and (17) was omitted. The results presented here take it into account.

$$+\int_{R_0}^{R_1}\int_{-\infty}^{\tau_1(r)} q(r,\tau_0)\left[(\vec{D}\cdot\vec{\gamma}_0)(\vec{n}_0\cdot\vec{D})+(a^2-|V_0|^2)(\vec{n}_0\cdot\vec{D})\right] d\tau_0 dr$$
$$-4\pi a^2|D|^3\left[1-\frac{\vec{V}_0\cdot\vec{D}}{a|D|}\right]^2$$

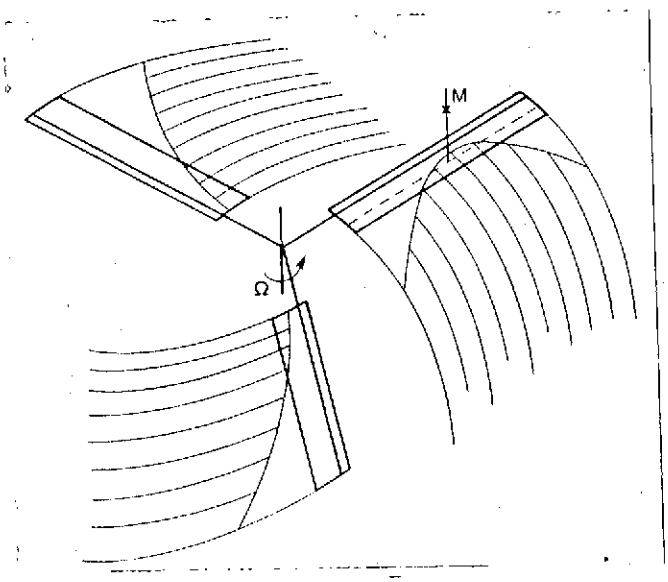

Fig. 8.

In the case of the three-/3-6 blade helicopter shown in Fig. 8, it is necessary to integrate over the three wake sheets created by the three lift lines. The interactions of one blade with the other also taken into account, in formula (17) τ_1 depends on r and one integrates in the portion of the sheets limited by the line $\tau_1(r)$ extending to infinity. Fig. 8 gives a good idea of the domains of integration (hachured area).

II. Method of Numerical Computation

We propose to apply the linearized theory to propellers and helicopters in permanent motion, i.e., when lift and blade motion are periodic functions of azimuth.

In order to do this lift will be expanded in a given basis of functions and the disturbance velocity created by each of these base functions will be determined. We will then seek the combination of base functions permitting the verification of the velocity conditions perpendicular to a certain number of points distributed on the blades for azimuth values.

We will see below that the disturbance velocity corresponding to each of the base functions actually depends only on the case of flight, forward and rotation velocities, and the plane shape of the blades. It does not depend on other blade characteristics, twist, collective pitch, rigidity. With the same computations, one can thus express conditions at the different limits, changing the combination of base functions, which requires only a few supplementary computations.

II,1. Representation of Lift

A propeller or helicopter blade will be diagramatically represented by a lifting segment situated in the forward quarter. Designating by r the distance of a blade section to the axis of rotation and by F(t,r) the integral of the pressures on this section, one has $F(t,r) = \int_{\text{chord}} \Delta p dx$. The elemental section is replaced by an intensity doublet $q(t,r) = \frac{F(t,r)}{\rho\infty}$ situated at a distance r from the axis.

Assuming that the regime has been established, F(t,r) is a periodic function of t or of the local azimuth, $\Phi = \Omega t + \alpha(r)$. If one wishes to define F(t,r) at a fixed point r_i, F(t,r) can be expanded in a Fourier series:

$$F(t,r_i) = Z_i + \sum_{j=1}^{m} X_{ij} \cos j\left(\Omega t + \alpha_{(r_i)}\right) + \sum_{j=1}^{m} Y_{ij} \sin j\left(\Omega t + \alpha_{(r_i)}\right). \qquad (18)$$

Phase setting $\alpha(r_i)$ is introduced to take into account a possible setting of the time origin along the lifting line. In the case of a lifting line passing through the axis of rotation $\alpha(r_i)$ will be a constant.

Relation (18) takes only specific points (r_i) into account. In order to describe the evolution of lift along the blade, at

a given moment t, one can, for example, select n points r_i and seek to interpolate force between these points (Fig. 9), by analogy with the theory developed for the wing [6], points r_i are defined as being Gauss points for the weight function $\sqrt{1-\eta^2}$, $-1 \leq \eta \leq 1$, with $\eta = \dfrac{2r_i - R_1 - R_0}{R_1 - R_0}$. These points are optimum points for the wing.

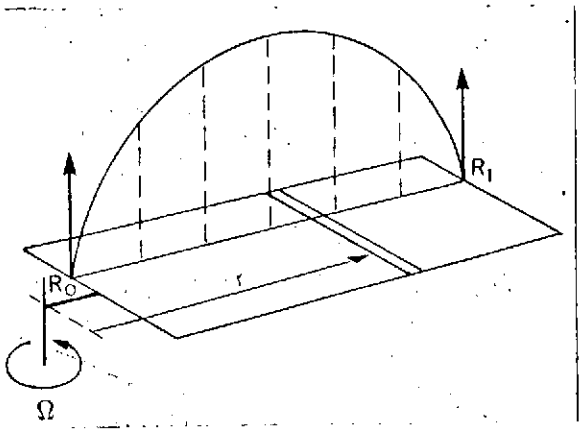

Fig. 9.

The interpolation between the points r_i is done by means of polynomials of Lagrange, polynomial $L_i(r)$ being the zero polynomial at points r_i for $j \neq i$ and equal to 1 for r_i (Fig. 10).

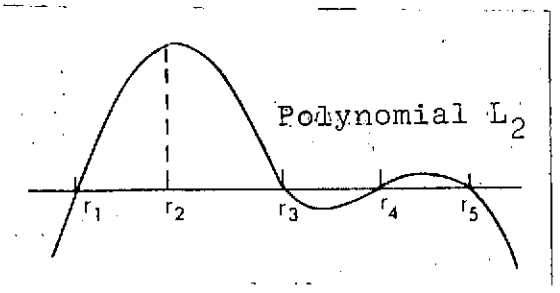

Fig. 10.

We will now take

$$F(t,r) = \sum_{i=1}^{n} L_i(r)\, F(t,r_i). \qquad (19)$$

which enables one to make F(t,r) /3-7 at the fixed moment t coincide with the values of F(t,r) computed at points r_i. In order to take into account the evolution of the aerodynamic loads in the course of time, $F(t,r_i)$ is replaced in (19) by the value furnished by expression (18):

$$F(t,r) = \sum_{i=1}^{n} Z_i L_i(r) + \sum_{i=1}^{n}\sum_{j=1}^{m} X_{ij} \cos j\left(\Omega t + \alpha(r)\right) L_i(r) + \sum_{i=1}^{n}\sum_{j=1}^{m} Y_{ij} \sin j\left(\Omega t + \alpha(r)\right) L_i(r). \qquad (20)$$

In (20) $\alpha(r_i)$ has been changed to $\alpha(r)$ for better consideration of the geometric definition of the lifting line. It has been determined that (20) agrees with the value of $F(t,r_i)$ yielded by (18) for $r = r_i$. Formula (20) can be used directly. However, at the two ends of the plate, lift varies very rapidly, and a large number of points r_i will be required to determine it if one was not careful to introduce in the expansion of $F(t,r)$ base functions whose behavior is the same as $F(t,r)$. In the case of a wing of finite span, theory anticipates that in the vicinity of the ends, the function $F(t,r)$ decreases as the square root of the distance to the lateral edges, proportionally to $\sqrt{1 - \eta^2}$.

Assuming that the neighboring conditions are satisfied for the blade, (20) will be multiplied by

$$\left| \sqrt{1-\eta^2}, \right| \text{ with } \eta = \frac{2r - R_1 - R_0}{R_1 - R_0}. \left|\right.$$

The model proposed for $F(t,r)$ then being closer to reality, less points r_i and therefore less unknowns Z_i, X_{ij}, Y_{ij} (i varying from 1 to n and j from 1 to m) will be required for the same accuracy. The intensity of the doublets situated on the lifting line is yielded by the formula

$$q(r,t) = \frac{\sqrt{1-\eta^2}}{\rho \infty} \left[\sum_{i=1}^{n} Z_i L_i(r) + \sum_{i=1}^{n} \sum_{j=1}^{m} X_{ij} \cos j(\Omega t + \alpha(r)) L_i(r) + \sum_{i=1}^{n} \sum_{j=1}^{m} Y_{ij} \sin j(\Omega t + \alpha(r)) L_i(r) \right]. \quad (21)$$

II,2. Collocation Method

Coefficients Z_i, X_{ij}, Y_{ij} are generally unknown, and the entire problem consists precisely in determining them. Formulas

(11) in incompressible flow and (17), for a compressible medium, in which q is replaced by the value furnished by expression (21), permit the calculation of the potential at any given point in space. Knowledge of the potential determines the disturbance velocity, and the collocation method consists in determining this velocity at a certain number of duly selected points. Blade interactions are taken into account very simply, extending the sums of formulas (11) and (17) to the wakes of all the blades with, on each occasion, the appropriate value for $\alpha(r)$.

For example, in the case of a three-blade helicopter:

$\alpha_1(r)$ for the first blade,

$\alpha_2(r) = \frac{2\pi}{3} + \alpha_1(r)$ for the second blade,

$\alpha_3(r) = \frac{4\pi}{3} + \alpha_1(r)$ for the third blade.

Definition of Collocation Points

The blade is likened to a lifting line. By analogy with the wing theory [5], one is led to place this line in the forward quarter and to determine the normal velocity induced along a line situated in the rear quarter.

More specifically, the collocation points will be placed at distances r_i from the axis of rotation, which are r_i have already served to determine the Lagrange polynomials. In order to justify linearization, it is assumed that each blade is turned back on its own wake, and that it is povided with slight motions in the direction perpendicular to this wake.

Under these conditions, the velocity component perpendicular to the blade is always low opposite the tangent component, /3-8

i.e., if the angle of attack is small, thus justifying linearization.

Velocity Induced by the Wakes at the Collocation Points

It is proposed to study the induced velocity component perpendicular to the blade, by the method given in reference [1]. The potential is calculated at two points P_1 and P_2 (Fig. 11) situated on one same perpendicular to the wake, at height h and h + Δf. The foot of this perpendicular passes through the collocation point. The velocity induced in the direction perpendicular to the wake is yielded by $W(h,\Delta h) = \frac{\phi(P_1) - \phi(P_2)}{\Delta h}$.

We wish to know $W(h;\Delta h)$ for h = 0 and Δh approaching 0. The presence of the term at $\frac{1}{|D|^2}$ in formula (11) and analogous terms in compressible flow make the computation of h = 0 difficult, since it is necessary to introduce a limit of integral (11) when h = 0. The numerical computations show however that $\phi(P)$ varies almost linearly with h over a very large distance. Only experience makes it possible to establish the compromise between the required accuracy for the induced velocity and the computation time necessary. For example, in the case of a blade 1.25 m long, 100 mm chord, h = 3.5 mm was chosen, or 3.5% of the chord, and Δh = 0.5 mm, or 0.5% of the chord.

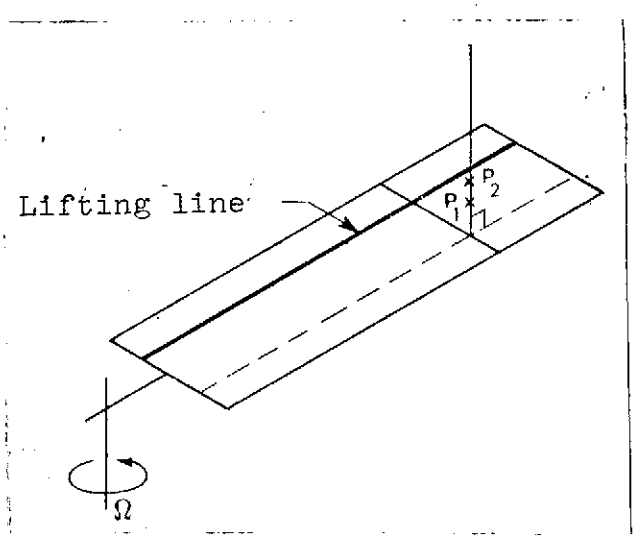

Fig. 11.

Computation of Aerodynamic Forces

The aerodynamic forces are determined by the unknown coefficient Z_i, X_{ij}, Y_{ij} of formula (21). The velocity perpendicular to the collocation points P_k, at moments t_1, will be expressed as a function of these coefficients and it will be written that it is equal to the projection of the velocity of point P_k normal to the blade.

The potential at point P at time t, results from the integrations in r and τ, explained by formulas (11) for the incompressible fluid and (17) for the compressible fluid. In these formulas, it is necessary to replace $q(r,\tau)$ by (21), and the vectors $\vec{D} = \overrightarrow{P_0P}$, $\overrightarrow{V_0}$, $\overrightarrow{\gamma_0}$ are determined by the trajectory of each blade and depend on r and on τ and on the height h, or $h + \Delta h$ above the wake.

When the computation for two points situated on the perpendicular to the wake passing through collocation point P_k at time t_1 is made it is possible to determine the finite difference which makes it possible to express $W(P_k,t_1)$ by algebraic equations of the form:

$$W(P_k, t_l) = \sum_{i=1}^{n} Z_i w_{i0}^{(0)}(P_k, t_l) + \sum_{i=1}^{n}\sum_{j=1}^{m} X_{ij} w_{ij}^{(1)}(P_k, t_l) + \sum_{i=1}^{n}\sum_{j=1}^{m} Y_{ij} w_{ij}^{(2)}(P_k, t_l). \qquad (22)$$

Coefficients w_{ij} are integrals in r and τ:
$w_{j0}^{(0)}(P_k,t_1)$ is the induced velocity at point P_k at moment t_1, when the intensity of the doublets is yielded by:

$$q(r) = \sqrt{1-\eta^2(r)}\, L_i(r).$$

$w_{ij}^{(1)}$ (P_k,t_l) is the induced velocity when the intensity of the doublets is yielded by

$$q(r,\tau)=\frac{\sqrt{1-\eta^2(r)}}{\rho_\infty}L_i(r)\cos j\ (\Omega\tau+\alpha(r)).$$

$w_{ij}^{(2)}$ (P_k,t_l) is the induced velocity when the intensity of the doublets is yielded by /3-9

$$q(r,\tau)=\frac{\sqrt{1-\eta^2(r)}}{\rho_\infty}L_i(r)\sin j\ (\Omega t+\alpha(r)).$$

The numerical computations consist in seeking the $w_{ij}^{(0)}$ $w_{ij}^{(1)}$ $w_{ij}^{(2)}$ which are derived from the integration over the combined wakes with more or less complicated but known functions.

Eq. (22) expresses the $W(P_k,t_l)$ as a function of Z_i, X_{ij}, Y_{ij}, by a matrix relation. By taking as many collocation points and times t_l as there are unknowns, the matrix of the w_{ij} is normalized and, after inversion, we obtain the matrix that expresses the unknowns Z_i, X_{ij}, Y_{ij} as a function of the normal velocities $W(P_k,t_l)$. Now, the latter are expressed directly as a function of parameters that define the motion and deformations of the blades by the condition of tangency.

Condition of Tangency of the Blade

At any point P whatsoever of a blade, at moment t, the perpendicular velocity induced by the wakes, W(P,t), must be equal to the projection on the perpendicular to the blade of the velocity of point P. The applications proposed in Chapters III and IV concern a propeller with rigidly mounted blades and a

helicopter comprising three hinged rigidly mounted blades whose motion is given by experience. The computation of W(P,t) in these two specific cases will be found below.

a) Case of a rigidly mounted propeller (Fig. 12):

OXYZ reference to an absolute coordinate system;

O'xyz coordinate system linked to the propeller axis;

point P of the blade is determined in polar coordinates in O'xyz by $(r, \Omega t + \alpha(r))$

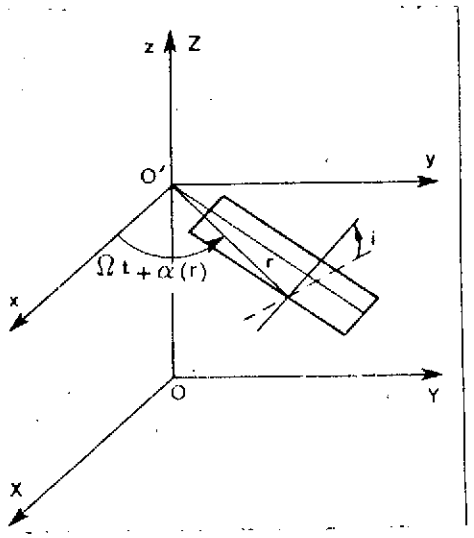

Fig. 12.

$$\vec{V_P} = \frac{d}{dt}\left(\overrightarrow{OO'} + \overrightarrow{O'P}\right)$$

$$\overrightarrow{O'P}\begin{cases} r\cos\left(\Omega t + \alpha(r)\right) \\ r\sin\left(\Omega t + \alpha(r)\right) \\ 0 \end{cases} \qquad \vec{V_P}\begin{cases} -r\Omega\sin\left(\Omega t + \alpha(r)\right) \\ r\Omega\cos\left(\Omega t + \alpha(r)\right) \\ U_\infty \end{cases}$$

in the absolute coordinate system the components of the perpendicular to the blade are n_x, n_y, n_z. By designating the setting of the airfoil at point P by i, we have:

$$\vec{n_p}\begin{cases} n_x = \sin i \sin\left(\Omega t + \alpha(r)\right) \\ n_y = -\sin i \cos\left(\Omega t + \alpha(r)\right) \\ n_z = \cos i \end{cases}$$

$$W(P,t) = \vec{V_p}\cdot\vec{n_p} = -r\Omega\sin i + U_\infty \cos i.$$

b) Case of the rigid-blade helicopter, with flapping hinge (Fig. 13):

The OXYZ coordinate system is an absolute coordinate system; O'xyz has axes parallel to those of the absolute coordinate system, O' being linked to the rotor head. The displacement O'

is defined by the velocity U_∞ and angle A situated in the OXZ plane.

O_1, the flapping hinge; its position is determined by r_0 and the angle $\Omega t + \alpha_0$. The coordinate system $O_1x_1y_1z_1$ is defined by Fig. 13, /3-10

O_1x_1 and O_1y_1 lie in the O'xy plane.

$O_2x_2y_2z_2$ is obtained from $O_1x_1y_1z_1$ by rotation of β around the axis O_1x_1. The coordinate system $O_2x_Ly_Lz_L$ is derived from $O_2x_2y_2z_2$ by rotation of i around axis O_2y_2. Axis O_2x_L defines the direction of zero lift of the airfoil. Rotation i expresses the twist of the blade and the collective pitch imposed thereon.

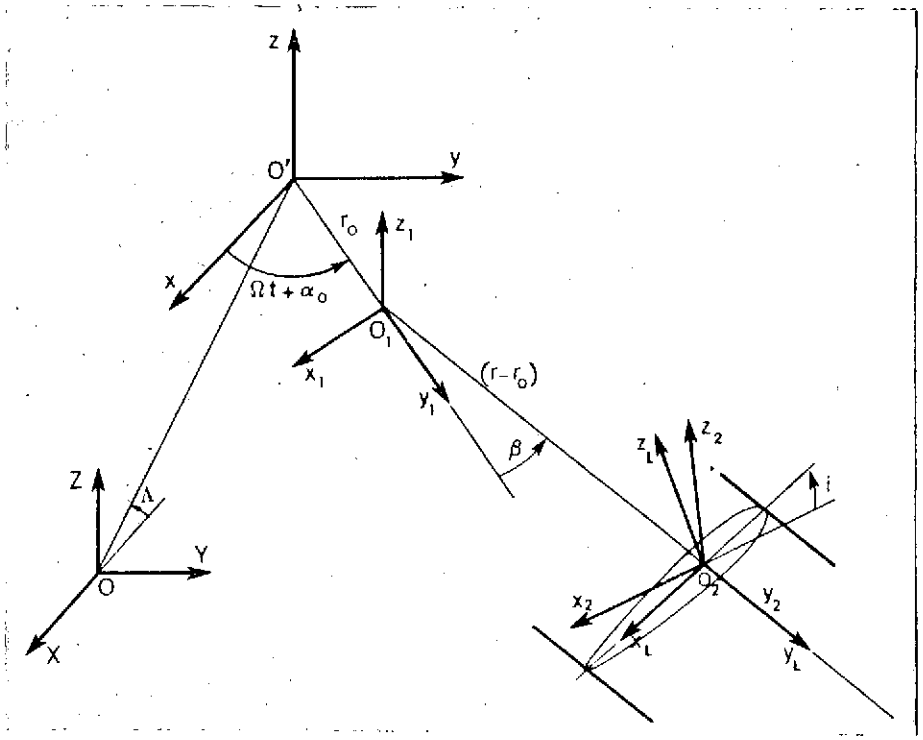

Fig. 13.

Any point P whatsoever of the blade is defined by its coordinates in $O_2x_Ly_Lz_L$ in the direction of zero lift, its coordinates are $(x_L, O_1, 0)$. Knowing r, $\beta(t)$, $\Omega t + \alpha_0$ it is possible to compute its velocity:

$$\vec{V}_P = \frac{d}{dt}\overrightarrow{OP} = \frac{d}{dt}\overrightarrow{OO'} + \frac{d}{dt}\overrightarrow{O'O_1} + \frac{d}{dt}\overrightarrow{O_1O_2} + \frac{d}{dt}\overrightarrow{O_2P}.$$

The perpendicular to the blade $\vec{n_p}$ at P is parallel to the axis O_2z_L. The scalar product of these two vectors yields the normal velocity:

$$W(P,t) = \vec{n_p}.\vec{V_p}.$$

The formulas for the change of base given below permit $\overrightarrow{OP}$ to be expressed in the absolute coordinate system. Their derivation with respect to time yielded by $\vec{V_p}$. The same formulas express $\vec{n_p}$ in the absolute coordinate system:

$$\begin{bmatrix} x_2 \\ y_2 \\ z_2 \end{bmatrix} = \begin{bmatrix} \cos i & O & \sin i \\ O & 1 & O \\ -\sin i & O & \cos i \end{bmatrix} \begin{bmatrix} x_L \\ y_L \\ z_L \end{bmatrix}$$

$$\begin{bmatrix} x_1 \\ y_1 \\ z_1 \end{bmatrix} = \begin{bmatrix} O \\ (r-r_0)\cos\beta(t) \\ (r-r_0)\sin\beta(t) \end{bmatrix} + \begin{bmatrix} 1 & O & O \\ O & \cos\beta(t) & -\sin\beta(t) \\ O & \sin\beta(t) & \cos\beta(t) \end{bmatrix} \begin{bmatrix} x_2 \\ y_2 \\ z_2 \end{bmatrix}$$

$$\begin{bmatrix} X \\ Y \\ Z \end{bmatrix} = \begin{bmatrix} -U_\infty \cos\Lambda t + r_0 \cos(\Omega t + \alpha_0) \\ r_0 \sin(\Omega t + \alpha_0) \\ U_\infty \sin\Lambda t \end{bmatrix} + \begin{bmatrix} \sin(\Omega t + \alpha_0) & \cos(\Omega t + \alpha_0) & O \\ -\cos(\Omega t + \alpha_0) & \sin(\Omega t + \alpha_0) & O \\ O & O & 1 \end{bmatrix} \begin{bmatrix} x_1 \\ y_1 \\ z_1 \end{bmatrix}$$

We obtain

$$\begin{aligned} W(P,t) = &-U_\infty \cos\Lambda \left[\sin i \sin(\Omega t + \alpha_0) - \sin\beta(t)\cos i \cos(\Omega t + \alpha_0)\right] \\ &+ U_\infty \sin\Lambda \cos\beta(t)\cos i - \Omega \sin i\left[r_0 + (r-r_0)\cos\beta(t)\right] - \sin\beta(t)\Omega x_L + (r-r_0)\dot{\beta}(t)\cos i. \end{aligned} \quad (23)$$

II,3. Geometric Definition of Wake /3-11

The linearized theory identifies wake, defined as the groups of points in space having velocity discontinuity properties with the geometric locus of the lifting segment moving in time.

This hypothesis, which is common in the aircraft wing theory is less justified in the case of a propeller or a helicopter. In these two applications, in effect, it will be necessary to take into account wake deformations in the computations of the coefficient $w_{ij}^{(k)}$. However, the main thing is to respect the distance between each blade and the wake sheet of the preceding blade, since it is the latter which, due to its proximity, has the greatest effect. That is why in numerical applications only the "cylindrical deformation" is taken into account. This is done by modifying the velocity component normal to the rotor disk: this component, which is equal to $U_\infty \sin\Lambda$ is replaced by $U_\infty \sin\Lambda + \nu$, where ν is a velocity correction parameter, generally small when compared to the points of the planes, and determined by the lift of the rotor. Thanks to this expedient, the lifting line describes a wake in much better agreement with the actual wake, at least in the vicinity of the disk.

It is evident that this parameter does not make it possible to take into account wake contraction, but the latter appears to have a negligible effect in the case of helicopters in forward flight, as shown especially by the results presented in [3].

It should be stated that ν does not affect the computation of normal velocities, $W(P_k,t_1)$ yielded by formula (23).

Remarks. The small motions and deformation of the blades modify the shape of these wakes, but they do affect the

deviation of the successive wakes when the periodic regime is attained, since in this case all wakes are modified in the same manner. Under these conditions coefficients $W_{ij}^{(k)}$ are independent, to about the second order, of the parameters defining these motions and vector $\vec{D} = \overrightarrow{P_0P}$ of formula (17) will be determined exclusively by the forward speed, the rotation speed and the tilt of the rotor, as long as the other motion parameters, such as the flapping angle, remain small. Thus, as long as the conicity of the rotor is small, the $w_{ij}^{(k)}$ can be computed assuming that $\beta(t) \equiv 0$.

Conversely, the small motions and deformations of the blades affect the computations of the velocities $W(P_k,t_1)$ normal to the collocation points (23).

III. Comparison of the Results Obtained by the Doublets Method and by the Vortex Method

The numerical application was carried out according to the principles developed above for an incompressible fluid. The case studied refers to a propeller turning at a speed of 30 revolutions per second and advancing at a speed of 111 m/sec. The diameter of the propeller was 2.5 m and that of the hub 0.5 m. Mach numer 0.85 is attained at the free end of the blade. As previously indicated, the cylindrical deformation introduced for the wake is determined by the momentum assuming an induced velocity distributed on the rotor [4]:

$$v = \frac{T}{2\pi\rho R^2\left[U_\infty + v\right]}\,; \quad t = \left|\text{ Total propeller thrust}\right.$$

R being the radius of the propeller and U_∞ the forward speed.

The wake permits the computation of the true induced velocity which is, to be sure, far from uniform. In the

applications studied, ν is equal to 1.5 m/sec at U_∞ to 111 m/sec and we actually have $\nu << U_\infty$.

When ν is small in the case of a propeller it is possible to take compressibility into account by means of the Prandtl correction. This amounts to multiplying the local incidences by $1/\sqrt{1 - M^2}$, M being the local Mach number. In the case of a propeller, the velocity U_∞ is perpendicular to the plane of the rotor. Lift does not depend on the azimuth and formula (22) is simplified, since X_{ij} and Y_{ij} are 0. We now only have to calculate $w_{io}^{(0)}(P_k,t)$ for any given time.

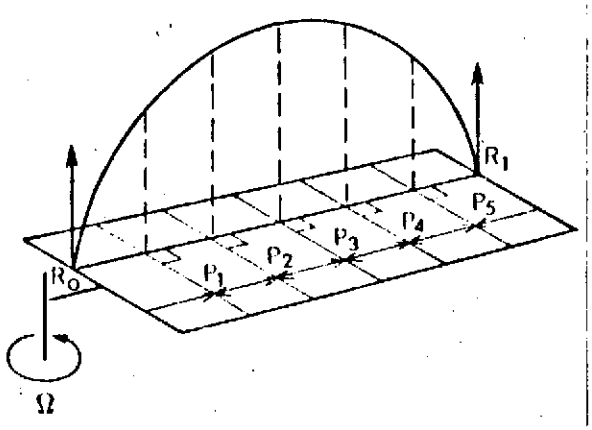

Fig. 14.

Assuming /3-12

$$n = 5,\ W(P_k, t) = \sum_{i=1}^{5} Z_i\, w_{io}^{(0)}(P_k, t),$$

we will seek in five points $P_1 \ldots P_5$ coefficients $w_{io}^{(0)}(P,t)$ obtained by integration over the wakes. The five points are situated on the line of their rear quarter of the blade. The latter is considered as falling back on its own wake. Point P_k is situated at the distance r_k of the rotation axis (Fig. 14). The r_k have already made is possible to define the Lagrange polynomials (Figs. 9 and 10).

For the purpose of comparison with the vortex method which is the most classical, a first computation was made with the formula of the incompressible doublet (11), and the effect of compressibility was introduced with the Prandtl correction.

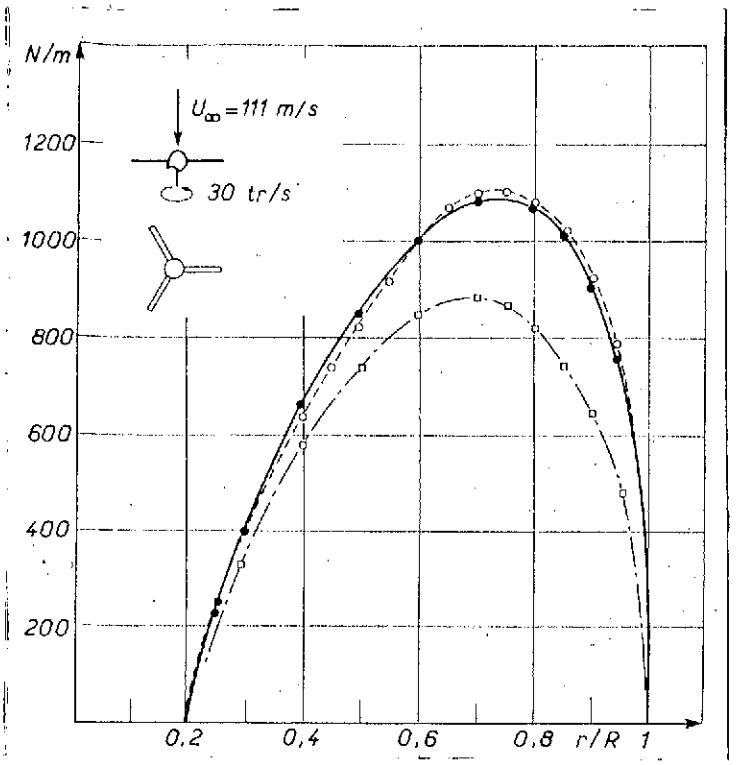

Fig. 15. Three-blade propeller

—●— SNIAS computation
--o-- Incompressible doublets (Prandtl approximation)
.—□—. Incompressible computation
r/R Normalized distance to the propeller axis. Mach = 0.85
N/m Lift per unit length

The results are shown in Fig. 15 and compared with the results computed at SNIAS (Societe Nationale Industrielle Aerospatiale) by R. Hirsch with the vortex method. In this computation the wake is represented by vortex arrays and the induced velocity is determined by the Biot and Savart law. But as this is only valid in the case of an incompressible fluid, the effect of compressibility can only be introduced by means of the Prandtl correction.

Fig. 15 represents the distribution of lift as a function of the radial coordinate.

It is observed that the results yielded by the vortex method and by the doublet method are virtually identical.

IV. Results in a compressible fluid

As the preceding numerical computation serves as a test to verufy the numerical integration methods used, the latter were applied to the doublet theory in a compressible medium.

The calculations made apply to:

1) The propeller studied above, which will permit a comparison between the direct computations and the corrected compressible theory computations.

2) A case of helicopter flight and the comparison between theory and the experimental data.

IV,1. Numerical Application in the Case of the Propeller

The integration and solution methods are copied from those used in an incompressible fluid. The results obtained are shown in Fig. 16. The curve marked "SNIAS computation;" is the same as the one in Fig. 15. It is obtained by a vortex method with a Prandtl correction. The curve marked "compressible doublets" respresents the direct computation by the doublet /3-13
method in a compressible fluid (formula (17)), and does not therefore involve corrections. For purposes of comparison, the third curve yields the results of computations made by the doublet method in an incompressible fluid without the Prandtl correction.

Examination of Figs. 15 and 16 show the good agreement of the three theoretical approaches and justifies the Prandtl correction in the case of the propeller.

IV,2. Numerical Application in the Case of the Helicopter Comparison Between Theory and Experiment

The existence of the experimental survey made at Modane, at the time of the July 1970 tests, with a S.N.I.A.S. experimental rotor permitted the comparison between theory and

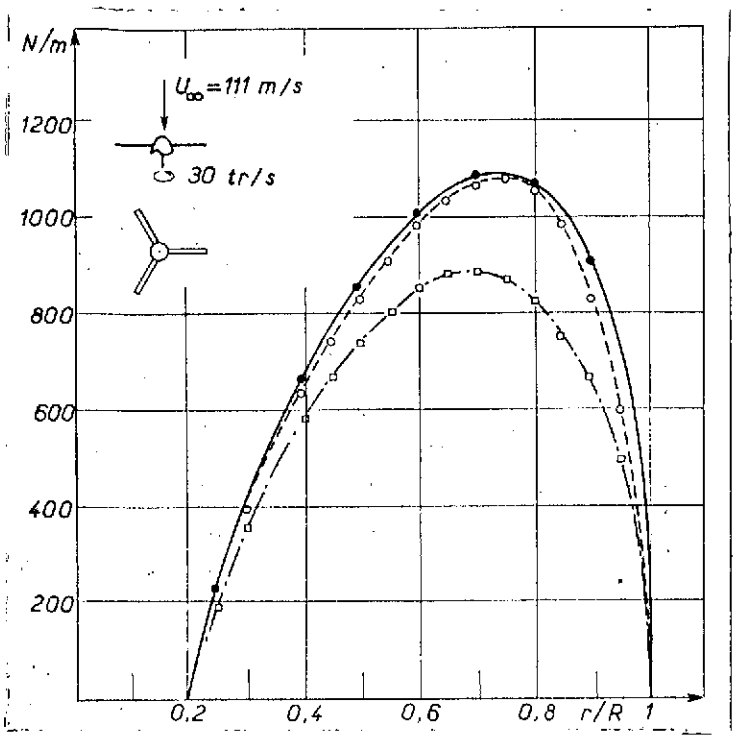

Fig. 16. Three-blade propeller.

—●— S.N.I.A.S. computation
--o-- Compressible doublets
·-□-· Uncorrected incompressible doublets
r/r Normalized distance to the propeller axis
N/m Lift per unit length

experiment in the case of helicopter flight compatable with the linearity conditions required by theory (Fig. 17). The low value of the forward motion ratio $\mu = 0.3$ determines an inversion circle with a relatively small diameter as compared to that of the rotor. The absence of a separated zone in the retreating blade was observed. The Mach number at the tip of the advancing blade is 0.78.

The pressure doublets break down according to formula (21), with $n = 5$ and $m = 5$, which yields 55 unknowns Z_i, X_{ij}, Y_{ij} which must be determined by 55 equations. Five equations can be written for each blade position; it is therefore necessary to compute the induced velocities for 11 blade positions, which will be taken equidistant and arranged as shown in Fig. 17. The normal velocity in the interior of the inversion circle is not low when compared with the tangential velocity, which foils the linearized theory, but lift is low because the resulting velocity is low. These considerations led us to replace the normal velocity conditions by the zero lift condition for the sections involved. The small area of the inversion circle in the example studied provides for this computation hypothesis.

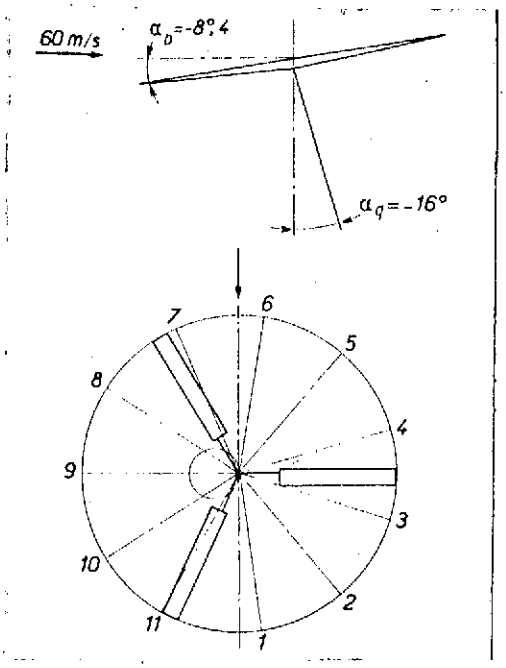

Fig. 17. Ω = 920 t/min, μ = 0.3, β = 1.22-7.55 cosψ.

The blades used could be considered as rigid with a very good approximation. A series of differentially mounted pressure sensors and placed in four different sections with r/R_1 = 0.52; 0.71; 0.855 and 0.952, permitted the measurement of

$$P_m(t) = \int_{\text{chord}} \frac{\Delta p(t)}{P_0} d\left(\frac{x}{c}\right)$$

(P_0 static pressure in the air flow, C chord of the blade).

The evolution of $P_m(t)$ is shown in Fig. 18 for the four sections. In the translation of the tangency condition, the motion of the blade is assumed to be known. It is taken as equal to the experimentally observed motion. The problem is thus reduced to the solution of a linear system of 55 equations with 55 unknowns. Fig. 18 presents the results obtained. The azimuth position, having as its origin the extreme rear position of the blade, is plotted in abscissa. The maximum error is situated in the vicinity of the 0° and 180° azimuths, which can be sought to be explained by the following facts:

1) The respective position of the lift segment and of the collocation line are linked to the pressure distribution along the airfoil; it is possible that the importance of the radial velocity component for the zones approaching 0° and 180°, lead to a systematic error by changing the pressure distribution;

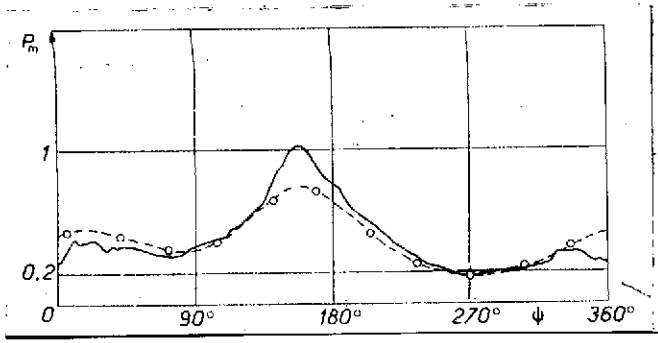

Fig. 18 a. Distance to the axis r/R = 0.52

——— Experiment

--o-- Doublets.

$P_m = \int_0^1 \frac{\Delta p}{p_0} d\left(\frac{x}{c}\right)$.

ψ = azimuth of the blade.

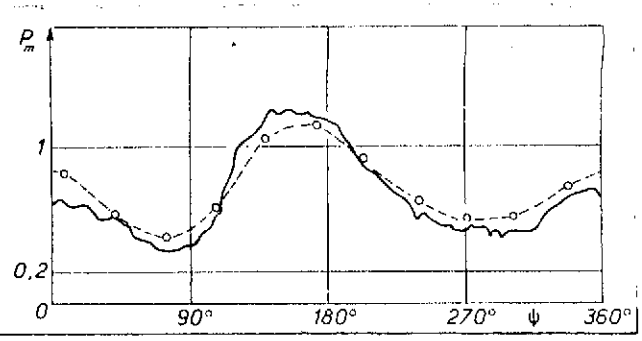

Fig. 18 b. Distance to the axis r/R = 0.71

——— Experiment

--o-- Doublets

$P_m = \int_0^1 \frac{\Delta p}{p_0} d\left(\frac{x}{c}\right)$.

ψ = azimuth of the blade.

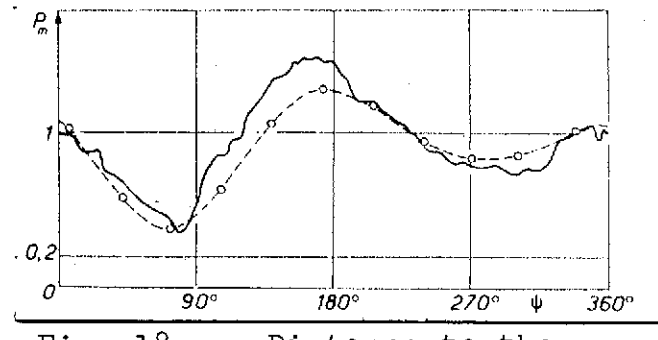

Fig. 18 c. Distance to the axis r/R = 0.855

——— Experiment

--o-- Doublets.

$P_m = \int_0^1 \frac{\Delta p}{p_0} d\left(\frac{x}{c}\right)$.

ψ = azimuth of the blade.

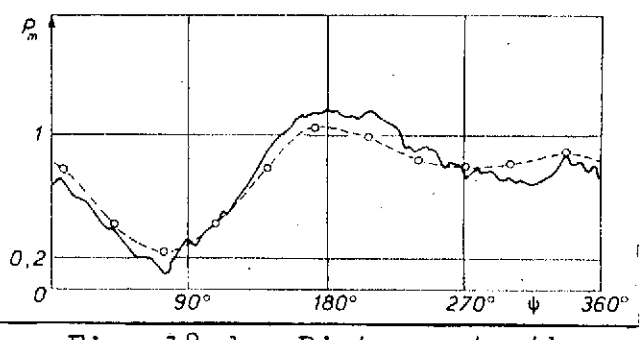

Fig. 18 d. Distance to the axis r/R = 0.952

——— Experiment

--o-- Doublets

$P_m = \int_0^1 \frac{\Delta p}{p_0} d\left(\frac{x}{c}\right)$.

ψ = azimuth of the blade.

2). The existence of vortices issuing from the hub and the wing fittings is negligible, and this can be important in the vicinity of the 0° azimuth.

Harmonic Analysis of Results

Fig 19 shows the evolution of the static component and of the harmonic components of lift as a function of the reduced distance to the axis of rotation.

The views at the left show the evolution of the components in cosine and those at the right in sine:

$$P_m\left(t, \frac{r}{R_1}\right) = A_0\left(\frac{r}{R_1}\right) + A_1\left(\frac{r}{R_1}\right)\cos \Omega t + B_1\left(\frac{r}{R_1}\right)\sin \Omega t + A_2\left(\frac{r}{R_1}\right)\cos 2\Omega t + \ldots$$

The origin of the times is determined by the passage of the blade past 0° azimuth. The upper harmonics of order four have not been shown because experience, as well as the computation made, show that their level is negligible. The agreement between theory and experiment is still good except for the cosine term of the first harmonic which is obtained by summation

/3-15

$$A_1\left(\frac{r}{R_1}\right) = \frac{2}{T}\int_{\text{période } T} P_m\left(\tau, \frac{r}{R_1}\right) \cdot \cos \Omega\tau \, d\tau.$$

The error in connection with this coefficient can be explained if the curves in Fig. 18 are taken into consideration. It will actually be seen that theory overestimates lift for ψ in the vicinity of 0° and that it underestimates it for ψ in the vicinity of 180°. Now for these azimuth values, $\cos\Omega\tau$ is respectively close to +1 and to - 1 and under these conditions

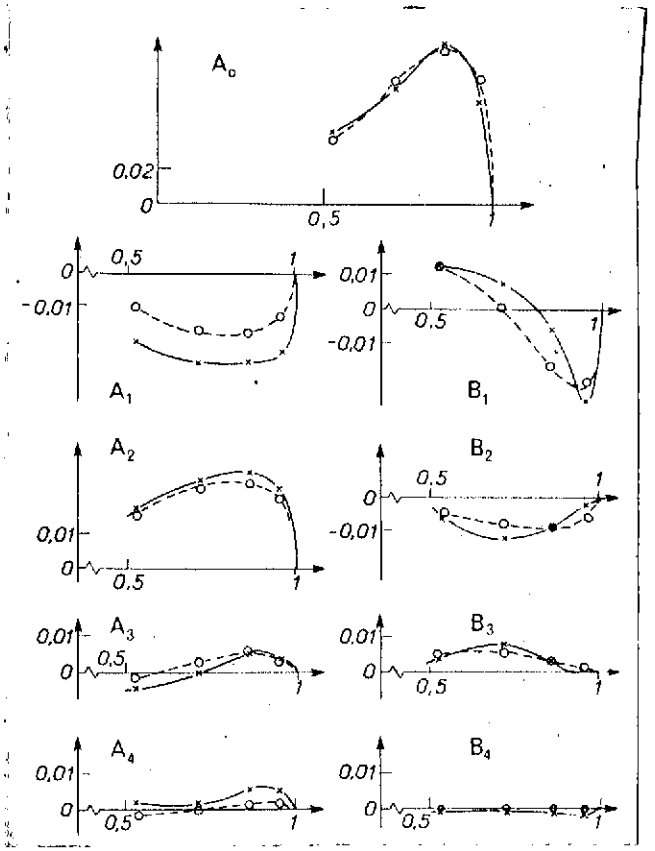

Fig. 19. r/R in abscissa.
—x— Experience
--o-- Theory

Harmonic analysis in ordinate
Ai = term in cosine
Bi = term in sine

the errors are compounded when the integral yielding A_1 is calculated.

This is no longer the case for $A_2(r/R_1)$ since the errors are multiplied by the terms in the vicinity of +1 and, being of opposite sign, they are compensated. The unfavorable case is reproduced for the coefficient of $\cos 3\Omega t$; Fig. 19 actually shows that the agreement is not so good for $A_3(r/R_1)$. Conversely, the good results obtained for the 90° and 270° azimuths (see Fig. 18) involve a good agreement for the terms at $\sin(k\Omega t)$ (see Fig. 19) since the maximum errors are multiplied in the summations of the harmonic analysis by small $\sin(k\Omega t)$. The results published in [3], already cited, present the same phenomenon of very important errors, particularly, with respect to term $A_1(r/R_1)$. These results originate in the use of a vortex method with a very elaborate wake deformation. This tends to prove that the errors in connection with terms A_1 and A_3, in our results, do not originate in the cylindrical deformation adopted for the wake, but probably originate in the schematization of the blade by a single lifting line, since this simplification is common to both methods.

Overall Performance of the Rotor

At the time of the test, the mean resultant of the aerodynamic forces exerted on the rotor were measured. The component along the rotor axis rose to 4682 N. Another test conducted under the same conditions, after removing the blades, yielded for the blade head and fittings 42 N, which yields 4640 N for the blades alone, neglecting the mutual interactions. Computations yield 4417 N, that is an error of 4.8%.

Examination of the curves in Fig. 18 show that it would have been useful to know the induced velocities in a number of azimuthal position greater than 11, which amounts to increasing the number m of harmonics studied. The description of the evolution of lift in time being better it is possible that results closer to experiment will be obtained.

V. Conclusion

The adjustment of the computation program in the compressible unsteady linear theory made it possible to reproduce the experimental results with a good degree of accuracy, in the case of a sufficiently sound flight which did not present due important separations or local incidences outside the inversion circle and its vicinities, where lift remains low. Since these results were obtained without any empirical correction on the basis of perfectly defined simplifying hypotheses regarding the position of the lifting line and other collocation points and regarding wake deformation and expression of the tangency condition, it is possible that experience may suggest corrections to improve this agreement in the area of flight where the linearized theory is still justified.

Manuscript submitted 14 January 1972.

REFERENCES

1. Dat, R., "Representation of a lifting line with a vibratory motion due to a line of acceleration doublets," Rech. Aérosp., No. 133, Nov-Dec. 1969.

2. Dat, R., "Aeroelastic vibrations -- second part -- unsteady aerodynamics; theory of the lifting surface," Cours École Nat. Sup. Aeron. Toulose, 1969.

3. Joglekor, M., and Loewy, R., "An actuator-disk analysis of helicopter wake geometric and the corresponding blade response," USA AVLABS, Technical Report 69-66, Dec. 1970.

4. Gessow, A., and Myers, C., Aerodynamics of the Helicopter, MacMillan Company, New York, 1952.

5. Dat, R., and Akamatsu, Y., "Representation of a wing or lifting lines; application to the computation of the interaction of two tandem wings," AGARD Conf. Proc. No. 80, Part 1, No. 5, 1971.

6. Williams, D. E., "Three-dimensional subsonic theory," AGARD Manual on Aeroelasticity, Vol. II.